JOC Article
pubs.acs.org/joc

Quantum-Mechanical Study of 10-R-9-borabicyclo[3.3.2]decane Alkene Hydroboration

Daniel H. Ess,* Jeremy Kister, Ming Chen, and William R. Roush*

Department of Chemistry, The Scripps Research Institute, Scripps Florida, Jupiter, Florida 33458

daniel@scripps.edu; roush@scripps.edu

Received August 10, 2009

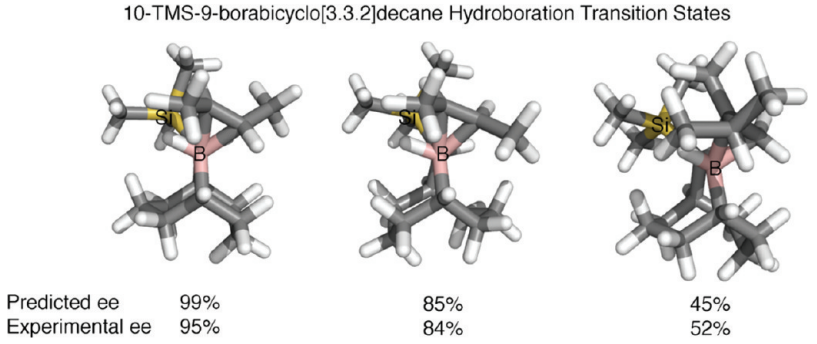

Density functional theory and correlated ab initio quantum mechanical methods were used to locate and analyze alkene hydroboration transition structures for 10-R-9-borabicyclo[3.3.2]decane reagents. Transition-state ensembles quantitatively modeled enantioselectivity for hydroboration of cis-, trans-, and *gem*-disubstituted alkenes in excellent agreement with experiment. The 10-R group and borabicyclo[3.3.2]decane ring conformation effects were analyzed to understand the origin of asymmetric selectivity.

1. Introduction

Brown and co-workers' use of diisopinocamphenylborane [$(Ipc)_2BH$] (**1a**, Chart 1) for alkene hydroboration−hydroxylation is a classic example of reagent-controlled asymmetric synthesis.[1] Although $(Ipc)_2BH$ induces over 99% enantiomeric excess (ee) upon reaction with cis-disubstituted alkenes, it gives quite poor ee for other types of substituted alkenes.[1,2] Masamune's reagent (**1b**) is highly effective for cis-, trans-, and trisubstituted alkenes, but not *gem*-disubstituted alkenes. However, it is not widely used due to the difficulty of its synthesis.[3] In 2008, Soderquist and co-workers showed that 10-substituted-9-borabicyclo-[3.3.2]decanes (**2a** and **2b**, Chart 1) react with a variety of substituted alkenes with good to high enantioselectivity (Chart 2).[4] For example, the reaction of **2a** or **2b** with *trans*-2-butene (**3**) results in alcohol products with greater than 95% ee. However, for *cis*-2-butene (**4**), only **2a** with a 10-trimethylsilyl (TMS) group results in high enantioselectivity (84% ee). Most novel about reagent **2a** is the induction of 52% ee for the hydroboration reaction of 1,1-disubstituted alkene **5** and 56% ee with alkene **6**. Although the 10-Ph reagent **2b** gives poor hydroboration enantioselectivity with alkenes **4** and **5**, it does induce 92% ee for reaction with alkene **6**. Soderquist and co-workers have also used the 10-substitution borabicylo[3.3.2]decane unit successfully for a variety of other asymmetric reactions,

(1) (a) Brown, H. C.; Zweifel, G. *J. Am. Chem. Soc.* **1961**, *83*, 486. (b) Brown, H. C.; Ayyangar, N. R.; Zweifel, G. *J. Am. Chem. Soc.* **1962**, *84*, 4341. (c) Brown, H. C.; Ayyangar, N. R.; Zweifel, G. *J. Am. Chem. Soc.* **1962**, *84*, 4343. (d) Brown, H. C.; Ayyangar, N. R.; Zweifel, G. *J. Am. Chem. Soc.* **1963**, *85*, 2072. (e) Brown, H. C.; Zweifel, G. *J. Am. Chem. Soc.* **1964**, *86*, 393. (f) Zweifel, G.; Ayyangar, N. R.; Brown, H. C. *J. Am. Chem. Soc.* **1964**, *86*, 397. (g) Zweifel, G.; Ayyangar, N. R.; Brown, H. C. *J. Am. Chem. Soc.* **1964**, *86*, 1071. (h) Zweifel, G.; Ayyangar, N. R.; Munekata, T.; Brown, H. C. *J. Am. Chem. Soc.* **1964**, *86*, 1076. (i) Brown, H. C.; Singaram, B. *Pure Appl. Chem.* **1987**, *59*, 879. (j) Brown, H. C.; Singaram, B. *Acc. Chem. Res.* **1988**, *21*, 287.

(2) (a) Thomas, S. P.; Aggarwal, V. K. *Angew. Chem., Int. Ed.* **2009**, *48*, 1896. (b) Brown, H. C.; Schwier, J. R.; Singaram, B. *J. Org. Chem.* **1978**, *43*, 4397. (c) Brown, H. C.; Singaram, B. *J. Am. Chem. Soc.* **1984**, *106*, 1797. (d) Brown, H. C.; Jadhav, P. K.; Mandal, A. K. *J. Org. Chem.* **1978**, *43*, 5074.

(3) Masamune, S.; Kim, B. M.; Petersen, J. S.; Sato, T.; Veenstra, S. J.; Imai, T. *J. Am. Chem. Soc.* **1985**, *107*, 4549.

(4) Gonzalez, A. Z.; Román, J. G.; Gonzalez, E.; Martinez, J.; Medina, J. R.; Matos, K.; Soderquist, J. A. *J. Am. Chem. Soc.* **2008**, *130*, 9218.

Published on Web 10/13/2009 DOI: 10.1021/jo901737d

most notably asymmetric allyl- and crotylboration of aldehydes.[5]

CHART 1. Most Important Asymmetric Hydroboration Reagents

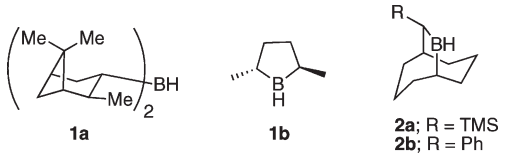

CHART 2. Reported Hydroboration Enantioselectivity (% ee) for Disubstituted Ethylenes[4]

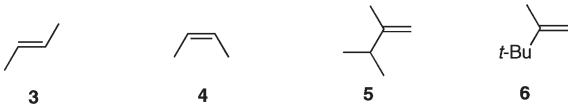

2a + **3** = 95 ee	**2a** + **4** = 84 ee	**2a** + **5** = 52 ee	**2a** + **6** = 56 ee
2b + **3** = 96 ee	**2b** + **4** = 32 ee	**2b** + **5** = 38 ee	**2b** + **6** = 92 ee

Several theoretical studies have established that the alkene hydroboration transition structure consists of a four-centered structure with simultaneous boron−carbon and hydrogen−carbon σ-bond formation (Scheme 1).[6] Because of the involvement of the unoccupied boron p-orbital, both π- and σ-interactions mix into this transition state, avoiding a high-energy four-centered four-electron addition process. This results in a transition structure with significant π-complex character.[7] For BH_3 addition to ethylene in the gas phase, there is also a weak pretransition state π-complex. Although the transition states for BH_3 addition to alkenes have been extensively explored, there are surprisingly few calculations of transition structures involving complex hydroboration reagents.[8] The most notable hydroboration transition structure was reported by Houk and co-workers over two decades ago using parametrized molecular mechanics for $(Ipc)_2BH$ addition to ethylene.[9]

SCHEME 1. Generalized Reaction Coordinate Structures for Alkene Hydroboration

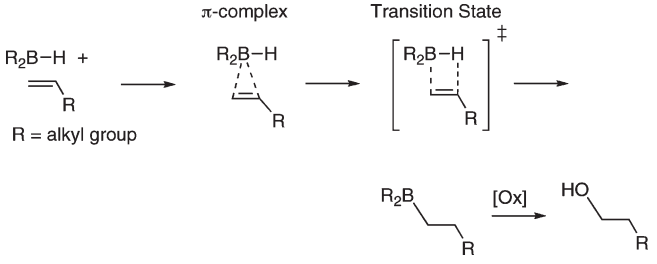

Oyola and Singleton have recently shown that transition-state theory overestimates anti-Markovnikov/Markovnikov regioselectivity for BH_3 addition to alkenes.[10] A classical trajectory study using direct dynamics starting with structures prior to the π-complex matched very well with the experimental regioselectivity. The success of dynamics calculations to predict regioselectivity is the result of a barrierless and exothermic π-complex that does not thermally equilibrate before the transition state for B−H bond addition.[10] In contrast, the dialkylborane reactions explored in this study have B−H bond addition barriers significantly higher than those of separated reactants. Therefore, normal thermal population and activation should dominate, and traditional transition-state theory is expected to sufficiently model selectivity.

The purpose of this contribution is to quantitatively model transition states and enantioselectivity for the hydroboration of disubstituted alkenes by the Soderquist boranes **2a** and **2b** with the goal of understanding the origin of asymmetric induction. Paramount to understanding enantioselectivity is deciphering the role of the 10-R group (TMS and Ph) versus the borabicyclo ring conformation. Soderquist and co-workers have postulated that the borabicyclo-[3.3.2]decane ring conformation is critical in determining enantioselectivity. Their molecular mechanics optimizations suggested that differences in selectivity between reagents **2a** and **2b** is the result of opposite boat/chair borabicyclo-[3.3.2]decane ring conformations (Chart 3); the long C−$SiMe_3$ bond in **2a** favors conformation 2 (**CF2**) with the boat side (7-position methylene) of the borabicyclo ring syn to the TMS group, while the shorter C−Ph bond favors conformation 1 (**CF1**) with the chair side (3-position methylene) syn to the 10-Ph group. Consequently, according to their analysis the 10-TMS group in **2a** is responsible for the major directing interactions, while in **2b** the 3-position methylene exerts a so-called "α-directive effect" that enhances π-facial selectivity for reactions with trans-substituted alkenes but decreases and reverses π-facial selectivity for reaction with cis alkenes.

CHART 3. Proposed Enantioselectivity Model by Soderquist and Co-workers

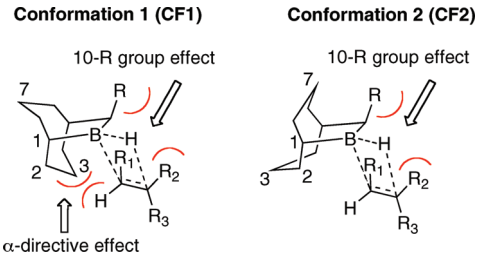

2. Computational Methodology

All density functional calculations were performed in Jaguar 7.0/7.5,[11] and all ab initio and composite method calculations

(5) (a) Canales, E.; Prasad, K. G.; Soderquist, J. A. *J. Am. Chem. Soc.* **2005**, *127*, 11572. (b) Burgos, C. H.; Canales, E.; Matos, K.; Soderquist, J. A. *J. Am. Chem. Soc.* **2005**, *127*, 8044. (c) Lai, C.; Soderquist, J. A. *Org. Lett.* **2005**, *7*, 799. (d) Gonzalez, A. Z.; Canales, E.; Soderquist, J. A. *Org. Lett.* **2006**, *8*, 3331. (e) Hernandez, E.; Burgos, C. H.; Alicea, E.; Soderquist, J. A. *Org. Lett.* **2006**, *8*, 4089. (f) Gonzalez, A. Z.; Soderuist, J. A. *Org. Lett.* **2007**, *9*, 1081. (g) Román, J. G.; Soderquist, J. A. *J. Org. Chem.* **2007**, *72*, 9772. (h) Soto-Cairoli, B.; Soderquist, J. A. *Org. Lett.* **2009**, *11*, 401. (h) González, A. Z.; Román, J. G.; Soderquist, J. A. *J. Am. Chem. Soc.* **2009**, *131*, 1269. (i) Muñoz-Hernández, L.; Soderquist, J. A. *Org. Lett.* **2009**, *11*, 2571.

(6) (a) Nagase, S.; Ray, N. K.; Morokuma, K. *J. Am. Chem. Soc.* **1980**, *102*, 4536. (b) Dewar, M. J. S.; McKee, M. L. *J. Am. Chem. Soc.* **1978**, *100*, 7499. (c) Clark, T.; Schleyer, P. v. R. *J. Organomet. Chem.* **1978**, *156*, 191.

(7) Nelson, D. J.; Cooper, P. J. *Tetrahedron Lett.* **1986**, *27*, 4693.

(8) Hommes, N. J. R. v. E.; Schleyer, P. v. R. *J. Org. Chem.* **1991**, *56*, 4074.

(9) (a) Houk, K. N.; Paddon-Row, M. N.; Rondan, N. G.; Wu, Y.-D.; Brown, F. K.; Spellmeyer, D. C.; Metz, J. T.; Li, Y.; Loncharich, R. J. *Science* **1986**, *231*, 1108. (b) Houk, K. N.; Rondan, N. G.; Wu, Y.-D.; Metz, J. T.; Paddon-Row, M. N. *Tetrahedron* **1984**, *40*, 2257. (c) Xuebao, W.; Li, Y.; Wu, Y.-D.; Paddon-Row, M. N.; Rondan, N. G.; Houk, K. N. *J. Org. Chem.* **1990**, *55*, 2601.

(10) Oyola, Y.; Singleton, D. A. *J. Am. Chem. Soc.* **2009**, *131*, 3130.

(11) (a) *Jaguar, version 7.0*, Schrodinger, New York, 2007. (b) *Jaguar, version 7.5*, Schrodinger, New York, 2009.

were performed in Gaussian 03.[12] All reactant and transition structures were optimized using B3LYP/6-31G(d,p) hybrid-density functional theory.[13] Energies of these structures were also evaluated using the spin-component scaled-MP2 (SCS-MP2)/6-31G(d,p)[14] method. This model of chemistry was chosen because it successfully models short-range (opposite spin) and static (same spin) correlation effects, and several studies have shown it to give comparable energies to CCSD(T) theory. In addition, SCS-MP2 also gives the dimethylborane−ethylene hydroboration activation barrier in close agreement with multi-component methods such as CBS-QB3,[15] G3,[16] and G3B3,[17] whereas B3LYP predicts slightly too high of barriers (see the Supporting Information). Enthalpy and free energy corrections were applied at 298 K using the B3LYP/6-31G(d,p) values. Diethyl ether (ε = 4.335, radius probe = 2.74) implicit free energy of solvation corrections were applied using the Poisson−Boltzmann solvation model. All geometrical data was obtained using Molden.[18] All transition-structure figures were generated using pymol.[19]

As discussed later, there are multiple competitive transition structures due to several borabicyclo ring conformations for hydroboration of alkenes by **2a** and **2b** leading to both the favored and unfavored product enantiomers. Therefore, the predicted enantiomeric excess was calculated on the basis of an approximate transition-state ensemble. Friesner and co-workers have recently used a similar analysis for alkene epoxidation reactions.[20] Asymmetric selectivity is the result of different rates of formation for each enantiomer. The observed enantiomeric excess (ee) is the difference between the rate of formation of the favored and unfavored enantiomer relative to the total rate (eq 1). Application of traditional transition-state theory (Eyring equation) with the assumptions of equivalent pre-exponential factors gives eqs 2 and 3.

$$\text{selectivity (ee)} = \frac{\text{rate}_{\text{favored}} - \text{rate}_{\text{unfavored}}}{\text{totalrate}_{(\text{favored+unfavored})}} \tag{1}$$

$$\frac{e_{\text{favored}}^{-(\Delta G^{\ddagger}/RT)} - e_{\text{unfavored}}^{-(\Delta G^{\ddagger}/RT)}}{e_{\text{favored}}^{-(\Delta G^{\ddagger}/RT)} + e_{\text{unfavored}}^{-(\Delta G^{\ddagger}/RT)}} \tag{2}$$

$$\frac{e^{-(\Delta\Delta G^{\ddagger}/RT)} - 1}{e^{-(\Delta\Delta G/RT)} + 1} \tag{3}$$

$$\Lambda \approx \sum_{n} e^{(-\Delta G/RT)} \tag{4}$$

$$\Delta\Delta G = -RT \ln \Lambda_{\text{favored}} + RT \ln \Lambda_{\text{favored}} \tag{5}$$

A transition-state ensemble for both favored and unfavored enantiomeric pathways was used to compute the free energy difference ($\Delta\Delta G^{\ddagger}$) between pathways. Electronic energy or enthalpy may also be used in place of $\Delta\Delta G^{\ddagger}$ under the assumptions of equivalent enthalpy and/or $-T\Delta S$ corrections. The ensemble was approximated as the Boltzmann-weighted partition function (Λ, eq 4) over all unique transition states that lead to the favored and unfavored enantiomers. Most ensembles were limited to three unique transition states (n = 3). The difference between these ensembles, eq 5, can then be inserted into eq 3 to give the predicted ee.

3. Results and Discussion

10-R-9-borabicyclo[3.3.2]decane Ground-State Conformations. To begin, Figure 1 shows the possible ground-state conformations of the 10-R-9-borabicyclo[3.3.2]decane ring for **2a** and **2b**.[21] Although ground-state conformations are not important for asymmetric selectivity, each of these conformations exists as a unique starting point for transition structures for addition to alkenes. Table 1 gives the relative energies for the four possible ring conformations. For **2a** and **2b**, all methods predict structure **CF1** to be lowest in energy. In this conformation the 3-position methylene group is directed up toward the 9,10-borabicylo bridge, while the 7-position methylene group is directed down to avoid interaction with the 10-R group. Conformation **CF2** with the 7-position methylene oriented toward the 10-R group is also low in energy and on average only ~1 kcal/mol higher than **CF1**. The closest $SiMe_3$ to the 7-position methylene group contact distance in **2a-CF2** is 2.249 Å, which is only a slightly larger contact distance than the 10-Ph group to the 7-position methylene group contact distance in **2b-CF2** of 2.239 Å (Figure 1). If both the 3- and 7-position methylene groups are oriented down (**CF3**) the relative energy increases by ~2 kcal/mol due to transannular repulsion. Conformation **2a-CF4** with both methylene groups up raises the energy by more than 4 kcal/mol. For reagent **2b** there is also the possibility for rotation of the 10-phenyl group by ~85° to give **2b-CF4**, which is ~1 kcal/mol higher than **2b-CF1**. The alternative boat/chair conformations of **2b-CF4** are

(12) *Gaussian 03, Revision C.02*: Frisch, M. J.; Trucks, G. W.; Schlegel, H. B.; Scuseria, G. E.; Robb, M. A.; Cheeseman, J. R.; Montgomery, J. A., Jr.; Vreven, T.; Kudin, K. N.; Burant, J. C.; Millam, J. M.; Iyengar, S. S.; Tomasi, J.; Barone, V.; Mennucci, B.; Cossi, M.; Scalmani, G.; Rega, N.; Petersson, G. A.; Nakatsuji, H.; Hada, M.; Ehara, M.; Toyota, K.; Fukuda, R.; Hasegawa, J.; Ishida, M.; Nakajima, T.; Honda, Y.; Kitao, O.; Nakai, H.; Klene, M.; Li, X.; Knox, J. E.; Hratchian, H. P.; Cross, J. B.; Bakken, V.; Adamo, C.; Jaramillo, J.; Gomperts, R.; Stratmann, R. E.; Yazyev, O.; Austin, A. J.; Cammi, R.; Pomelli, C.; Ochterski, J. W.; Ayala, P. Y.; Morokuma, K.; Voth, G. A.; Salvador, P.; Dannenberg, J. J.; Zakrzewski, V. G.; Dapprich, S.; Daniels, A. D.; Strain, M. C.; Farkas, O.; Malick, D. K.; Rabuck, A. D.; Raghavachari, K.; Foresman, J. B.; Ortiz, J. V.; Cui, Q.; Baboul, A. G.; Clifford, S.; Cioslowski, J.; Stefanov, B. B.; Liu, G.; Liashenko, A.; Piskorz, P.; Komaromi, I.; Martin, R. L.; Fox, D. J.; Keith, T.; Al-Laham, M. A.; Peng, C. Y.; Nanayakkara, A.; Challacombe, M.; Gill, P. M. W.; Johnson, B.; Chen, W.; Wong, M. W.; Gonzalez, C.; Pople, J. A. Gaussian, Inc., Wallingford, CT, **2004**.

(13) MPW1K energies are also given in the Supporting Information. (a) Lynch, B. J.; Fast, P. L.; Harris, M.; Truhlar, D. G. *J. Phys. Chem. A* **2000**, *104*, 4811. (b) Lynch, B. J.; Zhao, Y.; Truhlar, D. G. *J. Phys. Chem. A* **2003**, *107*, 1384. (c) Lynch, B. J.; Truhlar, D. G. *J. Phys. Chem. A* **2001**, *105*, 2936. (d) Lynch, B. J.; Truhlar, D. G. *J. Phys. Chem. A* **2002**, *106*, 842. (d) Lynch, B. J.; Truhlar, D. G. *J. Phys. Chem. A* **2003**, *107*, 3898.

(14) (a) Grimme, S. *J. Chem. Phys.* **2003**, *118*, 9095. (b) The SCS-MP2 method scales the electron correlation energy by 6/5 and 1/3 for spin-antiparallel and spin-parallel correlation energies. (c) Schwabe, T.; Grimme, S. *Acc. Chem. Res.* **2008**, *41*, 569.

(15) (a) Montgomery, J. A.; Frisch, M. J.; Ochterski, J. W.; Petersson, G. A. *J. Chem. Phys.* **1999**, *110*, 2822. (b) Nyden, M. R.; Petersson, G. A. *J. Chem. Phys.* **1981**, *75*, 1843. (c) Al-Laham, M. A.; Petersson, G. A. *J. Chem. Phys.* **1991**, *94*, 6081. (d) Petersson, G. A.; Tensfeldt, T. G.; Montgomery, J. A. *J. Chem. Phys.* **1991**, *94*, 6091. (e) Petersson, G. A.; Malick, D. K.; Wilson, W. G.; Ochterski, J. W.; Montgomery, J. A.; Frisch, M. J. *J. Chem. Phys.* **1998**, *109*, 10570. (f) Montgomery, J. A.; Frisch, M. J.; Ochterski, J. W.; Petersson, G. A. *J. Chem. Phys.* **2000**, *112*, 6532.

(16) (a) Pople, J. A.; Head-Gordon, M.; Fox, D. J.; Raghavachari, K.; Curtiss, L. A. *J. Chem. Phys.* **1989**, *90*, 5622. (b) Curtiss, L. A.; Jones, C.; Trucks, G. W.; Raghavachari, K.; Pople, J. A. *J. Chem. Phys.* **1990**, *93*, 2537.

(17) Baboul, A. G.; Curtiss, L. A.; Redfern, P. C.; Raghavachari, K. *J. Chem. Phys.* **1999**, *110*, 7650.

(18) Schaftenaar, G.; Noordik, J. H. *J. Comput. Aided Mol. Design* **2000**, *14*, 123.

(19) 2006 DeLano Scientific LLC.

(20) Schneebeli, S. T.; Hall, M. L.; Breslow, R.; Friesner, R. *J. Am. Chem. Soc.* **2009**, *131*, 3965.

(21) (a) The S-configuration of 2a and 2b was used throughout this study. Soderquist and co-workers utilized both R- and S-configurations in their study. See ref 4. (b) Sarotti and Pellegrinet have recently explored the conformational energies of allyl-10-R-9-borabicyclo[3.3.2]decanes. See: Sarotti, A. M.; Pellegrinet, S. C. *J. Org. Chem.* **2009**, *74*, 3562.

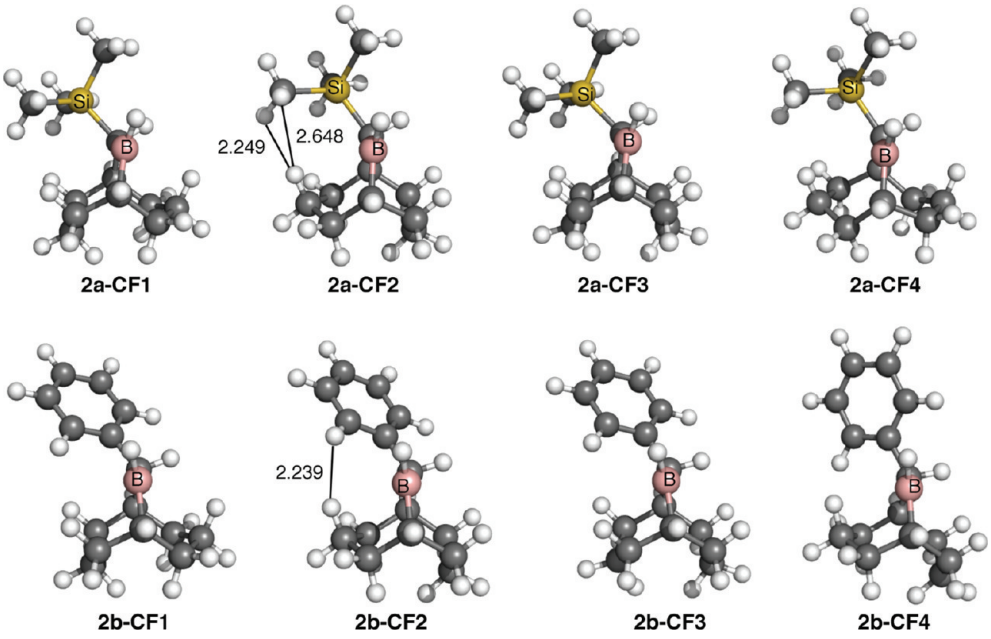

FIGURE 1. Ground-state 10-R-9-borabicyclo[3.3.2]decane ring conformations.

1−4 kcal/mol higher in energy. Although this phenyl group conformation is accessible in the ground state no transition structures were located with this phenyl group conformation.

TABLE 1. Relative Energies for 10-R-9-borabicyclo[3.3.2]decane Ring Conformations (kcal/mol)

		$\Delta E^{\ddagger}$		
	CF1	CF2	CF3	CF4
B3LYP/6-31G(d,p)				
2a	0.0	0.9	2.2	4.3
2b	0.0	0.7	2.2	0.8
SCS-MP2/6-31G(d,p)				
2a	0.0	1.3	3.0	4.6
2b	0.0	0.7	2.9	1.4

Each of these bicycloboranes can potentially form dimeric structures. For **2a**, the lowest energy borane dimer corresponds to [**2a-CF2**]$_2$ (see the Supporting Information for the structure). Significant intermolecular TMS group repulsions with the CH bridgehead and 2-position methylene group of the second borane leads to a weak binding energy (ΔE = −0.2 kcal/mol) and a highly endergonic dimeric structure (ΔG = 19.1 kcal/mol). In contrast, the flexibility of the 10-phenyl group to rotate in **2b** allows the borane dimers to have a much stronger dimeric interaction. "Cis" and "trans" dimers [**2b-CF1**]$_2$ have ΔE values of −16.2 and −16.3 kcal/mol. These large and nearly equal binding energies are consistent with the experimental observation of nearly equal amounts of dimeric "cis" and "trans" dimers from **2b** and no dimer formation from **2a**.

10-TMS-9-borabicyclo[3.3.2]decane Hydroboration of Ethylene. In addition to the four borabicyclo[3.3.2]decane ring conformations, ethylene can approach from the same or opposite side of the 10-R substituent, resulting in eight possible hydroboration transition structures. Figure 2 shows these transition structures for the reaction of **2a** with ethylene. Approach from the side opposite to the TMS group (**2a-TS1** through **2a-TS4**) is preferred by approximately a constant 4 kcal/mol over approach from the same side as the TMS group (**2a-TS5** through **2a-TS8**), indicating that the 10-TMS group rather than the borabicyclo[3.3.2]decane ring conformation dictates approach of ethylene (Table 2).

The lowest energy transition structure, **2a-TS1**, derives from the lowest energy ground-state conformation of **2a**. The B3LYP activation energy for **2a-TS1** is 12.5 kcal/mol above free reactants ($\Delta H^{\ddagger}$ = 13.9, $\Delta G^{\ddagger}$ = 26.2 kcal/mol; Table 2). The SCS-MP2 method predicts a moderately lower barrier of 8.0 kcal/mol. Transition structures **2a-TS2** (13.3 kcal/mol) and **2a-TS3** (13.8 kcal/mol) have energies within ∼1 kcal/mol of **2a-TS1**. Transition structures **2a-TS4** through **2a-TS8** are 3−8 kcal/mol above **2a-TS1** and were not considered further for substituted alkenes. Implicit diethyl ether free energy solvation corrections alter the barriers by less than 0.2 kcal/mol (see Table 2).

Geometrically, these hydroboration 4-centered addition transition structures are early along the reaction coordinate and have significant π-complexation character but do connect to the hydroboration addition adducts by IRC calculations. The B−H bond is stretched by an average of 0.02 Å compared to the ground-state bond length of 1.204 Å, while the C1−C2 ethylene bond is also slightly stretched to ∼1.360 Å from the ground state 1.331 Å. One geometrical probe of the degree of π character is the B−C1−C2 angle, which is 72° in **2a-TS1**.

10-TMS-9-borabicyclo[3.3.2]decane Hydroboration of *trans*-2-Butene. Experimentally, the reaction of **2a** with *trans*-2-butene (**3**) results in 95% ee.[4] Figure 3 shows the six most competitive transition structures for **2a** addition to **3**. In terms of reactivity, B3LYP predicts the hydroboration of alkene **3** with borane **2a** to have ∼5 kcal/mol higher barriers compared to ethylene, while SCS-MP2 predicts 1−3 kcal/mol higher barriers (Table 3). The higher activation barriers are the result of later transition structure reaction coordinate positions due to the steric congestion of the 10-TMS group. The forming B−C1 bonds are ∼0.1 Å

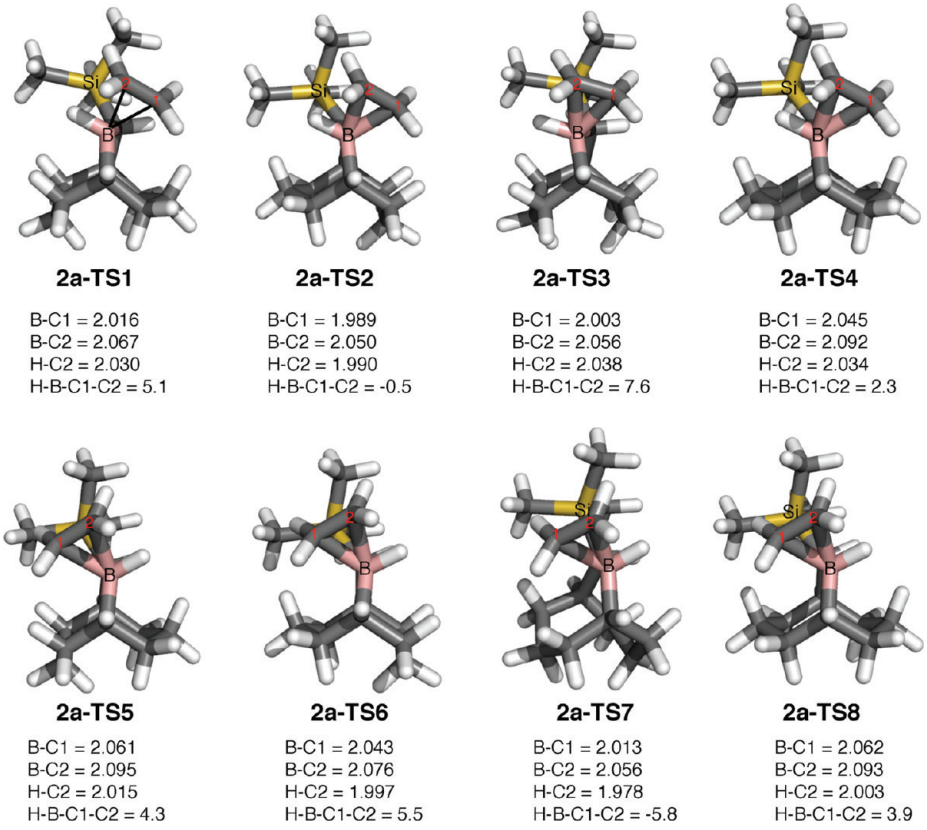

FIGURE 2. Eight lowest energy B3LYP/6-31G(d,p) transition structures for ethylene hydroboration by **2a**.

TABLE 2. Activation Energies, Enthalpies, and Free Energies (kcal/mol) for 2a Addition to Ethylene at 298 K

	$\Delta E^{\ddagger}$		$\Delta H^{\ddagger}$	$\Delta G^{\ddagger}$
structure	B3LYP/6-31G(d,p)	SCS-MP2/6-31G(d,p)	B3LYP/6-31G(d,p)	B3LYP/6-31G(d,p)
2a-TS1	12.5	8.0	13.9	26.2 (26.0)[a]
2a-TS2	13.3	8.7	14.6	27.2 (27.1)[a]
2a-TS3	13.8	9.4	15.3	28.0 (28.0)[a]
2a-TS4	17.0	12.5	18.3	30.0 (29.8)[a]
2a-TS5	15.6	11.4	17.1	30.2 (30.2)[a]
2a-TS6	15.5	10.8	17.0	30.3
2a-TS7	17.7	13.7	19.2	31.9
2a-TS8	19.4	15.0	20.9	33.6

[a]Diethyl ether solvation-corrected free energies are shown in parentheses.

shorter, and the forming H−C2 bonds are ∼0.2 Å shorter in comparison to the ethylene transition structures (compare Figures 2 and 3).

The favored hydroboration pathway is for BH addition to the *pro-S* face of **3**, which places the closest alkene methyl group away from the 10-TMS group. The lowest energy transition structure is **2a-3-TS2** with an activation energy of 17.5 kcal/mol. Here, SCS-MP2 predicts a significantly lower barrier of 9.1 kcal/mol. This transition structure has the same borabicyclo ring conformation that Soderquist and coworkers predicted and importantly does not correspond to the lowest energy ground state conformation (**2a-CF1**).[4] Structure **2a-3-TS2** is slightly lower in energy than **2a-3-TS1** ($\Delta E^{\ddagger}_{\mathrm{B3LYP}} = 17.8$ kcal/mol; $\Delta E^{\ddagger}_{\mathrm{SCS\text{-}MP2}} = 9.3$ kcal/mol) due to the close contact between the alkene methyl group and the 3-position bicyclo methylene group (2.101 Å) in **2a-3-TS1**. This interaction is more sterically crowded than the interaction between the TMS group and the 7-position methylene group (2.329 Å) in **2a-3-TS2**. The other important steric interaction in **2a-3-TS1** and **2a-3-TS2** is between the distal alkene methyl group and the 10-TMS group, which have similar distances of 2.442 Å and 2.418 Å, respectively. It is also important to note that on the free energy surface **2a-3-TS1** and **2a-3-TS2** have identical barriers with and without diethyl ether solvation correction.

For *pro-R* face hydroboration by **2a**, the lowest energy transition strucutre **2a-3-TS4** does have the same borabicyclo ring conformation as the lowest energy ground state (**2a-CF1**). This transition structure is 3.8 kcal/mol above **2a-3-TS2** due to the close contacts of the alkene methyl group with the 10-TMS group (2.078 and 2.434 Å). Transition structures **2a-3-TS5** and **2a-3-TS6** are ∼2 kcal/mol higher than **2a-3-TS4**. **2a-3-TS4** is lower in energy than **2a-3-TS5** because now the alkene methyl group is farther away from the 3-position borabicyclo methylene group (2.323 Å). The largest geometrical difference between the favored *pro-S* face addition and unfavored *pro-R* face addition is the H−B−C1−C2 dihedral angle. In **2a-3-TS1** through **2a-3-TS3** the dihedral angles range from −3° to −6°, while in **2a-3-TS4** through **2a-3-TS6** alkene **3** twists to ∼+15° to avoid interaction with the TMS group. This twisting alleviates some of the steric compression and is possible because the alkene vinyl hydrogen-10-TMS interaction remains at a distance of 2.340 Å.

The B3LYP energy difference between **2a-3-TS2** and **2a-3-TS4** is 3.8 kcal/mol. SCS-MP2 predicts a slightly larger energy difference of 4.5 kcal/mol. Transition structure **2a-3-TS1** is also highly competitive and has nearly the same

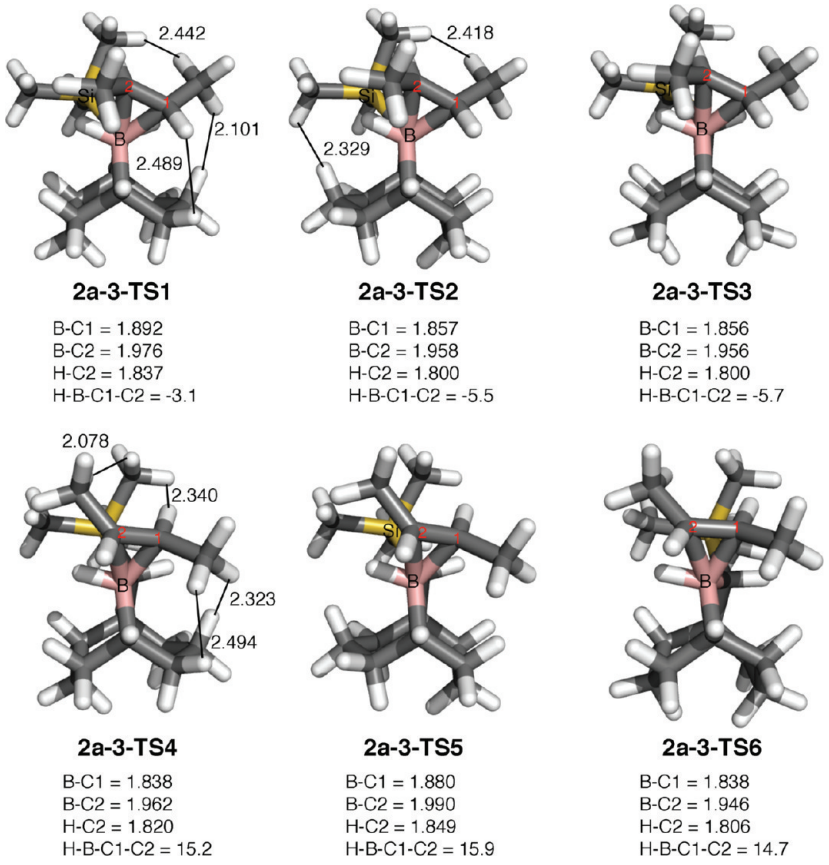

FIGURE 3. B3LYP/6-31G(d,p) hydroboration transition structures for **2a** with alkene **3**.

TABLE 3. Activation Energies, Enthalpies, and Free Energies (kcal/mol) for 2a Addition to 3 at 298 K

	$\Delta E^{\ddagger}$		$\Delta H^{\ddagger}$	$\Delta G^{\ddagger}$
structure	B3LYP/ 6-31G(d,p)	SCS-MP2/ 6-31G(d,p)	B3LYP/ 6-31G(d,p)	B3LYP/ 6-31G(d,p)
2a-3-TS1	17.8	9.3	19.0	33.8 (33.9)[a]
2a-3-TS2	17.5	9.1	18.8	33.8 (33.9)[a]
2a-3-TS3	19.7	12.3	21.1	35.6 (35.7)[a]
2a-3-TS4	21.3	13.6	22.6	37.8 (37.8)[a]
2a-3-TS5	23.0	15.4	24.4	39.6 (38.9)[a]
2a-3-TS6	22.9	15.1	24.3	39.1 (39.2)[a]

[a]Diethyl ether solvation-corrected free energies are shown in parentheses.

activation energy as **2a-3-TS2**. Because the energies of these transition structures are very close, the enantioselectivity was calculated by a transition-state ensemble based on a Boltzmann-weighted average over **2a-3-TS1** through **2a-3-TS3** for the favored enantiomeric pathway and **2a-3-TS4** through **2a-3-TS6** for the disfavored enantiomeric pathway. B3LYP and SCS-MP2 both predict 99% ee, an overestimate of the 95% ee reported experimentally (see Table 8).[22]

10-TMS-9-borabicyclo[3.3.2]decane Hydroboration of *cis*-2-Butene. For the reaction of **2a** with *cis*-2-butene (**4**) the barrier heights are very similar to that with trans-2-butene. The lowest energy transition structure for *pro-S* face hydroboration, **2a-4-TS1**, has a B3LYP activation energy of 17.0 kcal/mol ($\Delta E^{\ddagger}_{\text{SCS-MP2}}$ = 8.7 kcal/mol), see Figure 4 and Table 4. In this transition structure, and **2a-4-TS2**/**2a-4-TS3**, both alkene methyl groups are directed away from the 10-TMS group. Different from the reaction with alkene **3**, the lowest energy transition structure has the same borabicyclo[3.3.2]decane ring conformation as the lowest energy in the ground state (**2a-CF1**, Figure 1) ring conformation. This indicates that there is no severe repulsion between the 3-position methylene group and the methyl group of alkene **4** with an intramolecular distance of 2.510 Å. This is also the opposite of the borabicyclo[3.3.2]decane ring conformation proposed by Soderquist and co-workers, indicating that an α-directive effect is not a major directing force in the reaction of **2a** with alkene **4**. **2a-4-TS1** is lower in energy than **2a-4-TS2** because ring flip of the borabicyclo boat/chair conformation in **2a-4-TS1** decreases the distance between the 2-position methylene hydrogen and the methyl group to 2.114 Å in **2a-4-TS2** compared to a distance of 2.369 Å in **2a-4-TS1**.

The lowest energy transition structure for *pro-R* face hydroboration of **4** is **2a-4-TS4** with a barrier of 19.2 kcal/mol. Despite both methyl groups being oriented toward the bulky 10-TMS side of the bicyclo bridge, the energy difference between **2a-4-TS1** and **2a-4-TS4** is only 2.2 kcal/mol. This is a 2.3 kcal/mol lower than the $\Delta\Delta E^{\ddagger}$ value compared with the same transition structures for addition to alkene **3** where only one methyl group is direct toward the 10-TMS group. SCS-MP2 predicts a smaller $\Delta\Delta E^{\ddagger}$ value of 1.8 kcal/mol. Again, using a transition-state ensemble made up of the three most competitive transition structures for both the

(22) SCS-MP2 calculations with a larger basis set 6-311++G(d,p) lower the activation energies for all transition states by 1−3 kcal/mol. This larger basis set also predicts 99% ee. See the Supporting Information for comparison of basis sets.

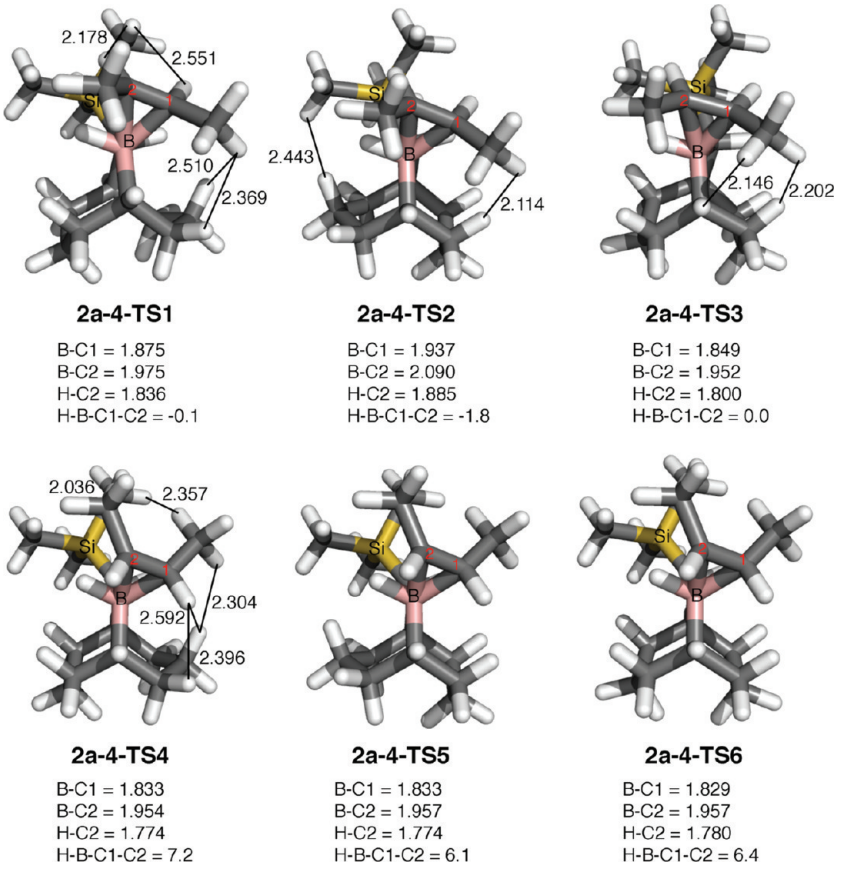

FIGURE 4. B3LYP/6-31G(d,p) hydroboration transition structures for **2a** with alkene **4**.

TABLE 4. Activation Energies, Enthalpies, and Free Energies for 2a Addition to 4 at 298 K

	$\Delta E^{\ddagger}$		$\Delta H^{\ddagger}$	$\Delta G^{\ddagger}$
structure	B3LYP/ 6-31G(d,p)	SCS-MP2/ 6-31G(d,p)	B3LYP/ 6-31G(d,p)	B3LYP/ 6-31G(d,p)
2a-4-TS1	17.0	8.7	18.2	32.9 (32.9)[a]
2a-4-TS2	18.5	10.5	19.8	34.2 (34.1)[a]
2a-4-TS3	18.9	10.8	20.2	34.9 (34.9)[a]
2a-4-TS4	19.2	10.5	20.3	35.7 (35.6)[a]
2a-4-TS5	19.6	11.2	20.8	36.1 (36.1)[a]
2a-4-TS6	21.6	14.3	22.8	37.8 (37.8)[a]

[a]Diethyl ether solvent-corrected free energies are shown in parentheses.

favored (**2a-4-TS1** through **2a-4-TS3**) and unfavored (**2a-4-TS4** through **2a-4-TS6**) enantiomeric reaction pathways, based on electronic energies, B3LYP overestimates the enantioselectivity with a predicted value of 94% ee compared to the experimental value of 84% ee. B3LYP $\Delta E^{\ddagger}$ values predict an 85% ee. SCS-MP2 $\Delta E^{\ddagger}$ values predict enantioselectivity induction at 89% ee.[23]

Why is there a lower selectivity for hydroboration of alkene **4** than **3**? In order to separate the selectivity based on each methyl group of alkenes **3** and **4**, the energy difference between **2a-3-TS2**/**2a-3-TS4** and **2a-4-TS1**/**2a-4-TS4** was compared with the reoptimized transition states after a single methyl group was deleted and replaced with hydrogen. These new transition structures correspond to the regioisomeric transition states for **2a** hydroboration of propene (Figure 5).

For the trans alkene **3**, Figure 5a shows that the methyl group closest to the TMS group induces 2.4 kcal/mol of selectivity between **2a-3-TS2**/**2a-3-TS4** while the methyl group near the borabicyclo 3-position methylene group induces 0.8 kcal/mol of selectivity. Importantly, the distal methyl group prefers to be close to the 10-TMS group rather than directed away from it. Therefore, both interactions work in conjunction to give large π-face selectivity. The same analysis was also performed on transition structures **2a-4-TS1** and **2a-4-TS4** (Figure 5b). Here, the methyl group interacting on the side closest to the TMS group induces a slightly larger energy difference of 2.8 kcal/mol. Again, the distal cis methyl group of alkene **4** is more stable by −0.9 kcal/mol when oriented toward the 10-TMS group rather than directed away from it. However, for this cis alkene these methyl group preferences work in opposition to each other and reduce the overall π facial selectivity.

The origin of the preference for the distal methyl group to orient toward the 10-TMS group is that the long C−$SiMe_3$ bond length (~1.91 Å) provides a hydrophobic cavity/pocket where the methyl group experiences less repulsion than when it is oriented away from the 10-TMS group where it encounters repulsion with the 2-position and 3-position methylene groups. In **2a-4-TS1**, the distance between the distal methyl group and the 2-position methylene group is 2.369 Å, while in **2a-3-TS4** this distance is 2.494 Å. Importantly, although the distal methyl prefers

(23) SCS-MP2/6-311++G(d,p) predicts lower activation energies for all transition states by ~1 kcal/mol and predicts and 86% ee. See the Supporting Information.

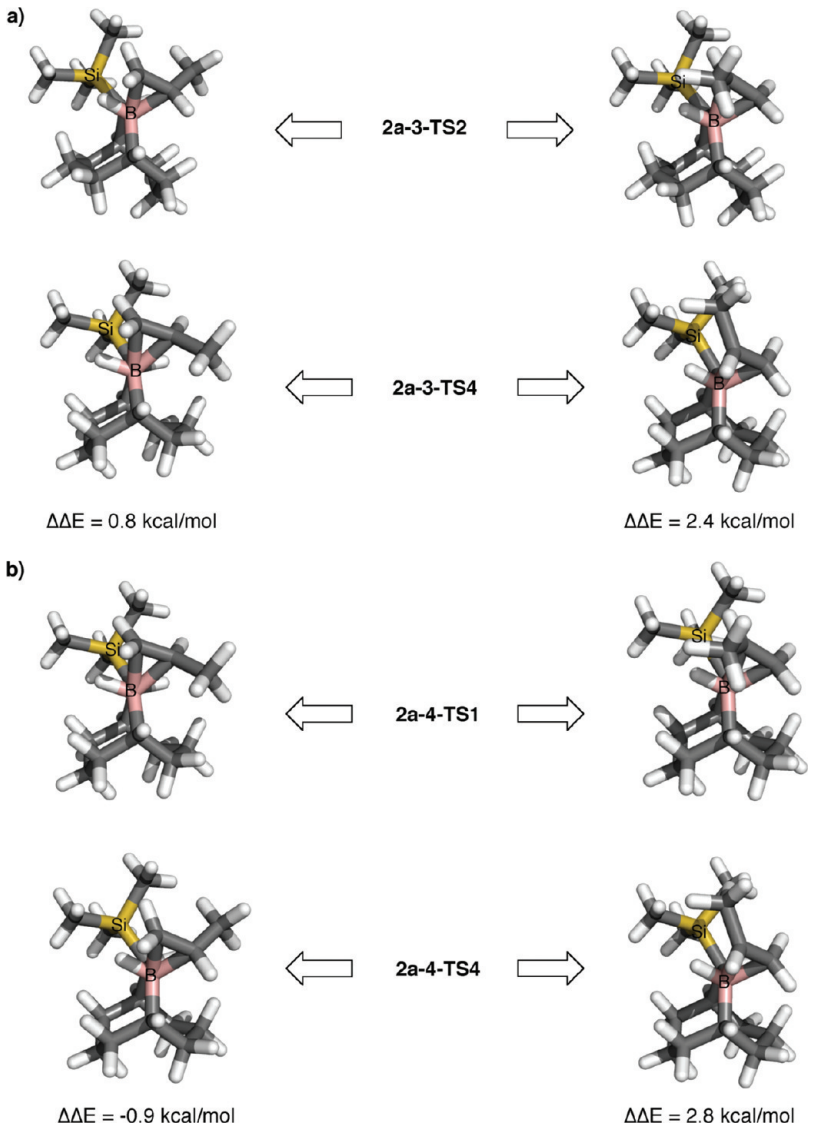

FIGURE 5. Energy difference between propene regioisomeric hydroboration transition structures. (a) Methyl group selectivity for hydroboration of alkene **3**. (b) Methyl group selectivity for hydroboration of alkene **4**.

to be oriented toward the 10-TMS side, the distance between this methyl group and the 3-position methylene group is shorter in **2a-4-TS4** (2.304 Å) than in **2a-4-TS1** (2.510 Å). This highlights the importance of an open cavity space by the TMS group and because of this 10-TMS binding pocket there is less alkene twisting in the transition structures with alkene **4** resulting in a H−B−C1−C2 dihedral angles of ~6°.

Alternative 10-R groups. To further explore the possibility of a 10-R group-alkene binding cavity, activation energies for hydroboration of alkenes **3** and **4** by hypothetical reagents **2c** (R = 10-*tert*-butyl) and **2d** (10-$SnMe_3$) were computed (Chart 4). These 10-R groups have different levels of steric congestion, and with C−CMe_3 and C−$SnMe_3$ bond lengths of ~1.58 and ~2.19 Å they provide very different spaces for a methyl group to fit into. Figure 6 shows the two lowest energy enantiomeric transition structures for the hydroboration of alkenes **3** and **4** with **2c** and **2d**. Table 5 reports the B3LYP activation parameters for all of the

CHART 4. Hypothetical Alkene Hydroboration Reagents Explored for Asymmetric Selectivity and Predicted Enantiomeric Excess

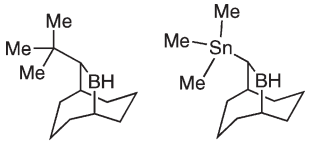

2c **2d**

2c + **3** = 99% ee **2d** + **3** = 99% ee
2c + **4** = 99% ee **2d** + **4** = 20% ee

borabicyclo ring conformation transition structures. Based on all of these transition structures, the predicted ee values for **2c** hydroboration of alkene **3** are greater than 99%. The smallest energy difference between favored and unfavored enantiomeric pathways is 3.3 kcal/mol. For the reaction of **2c** with **4**, the smallest $\Delta\Delta E^{\ddagger}$ value is 3.6 kcal/mol. In accord with this value, the predicted ee is also greater than 99%. The higher

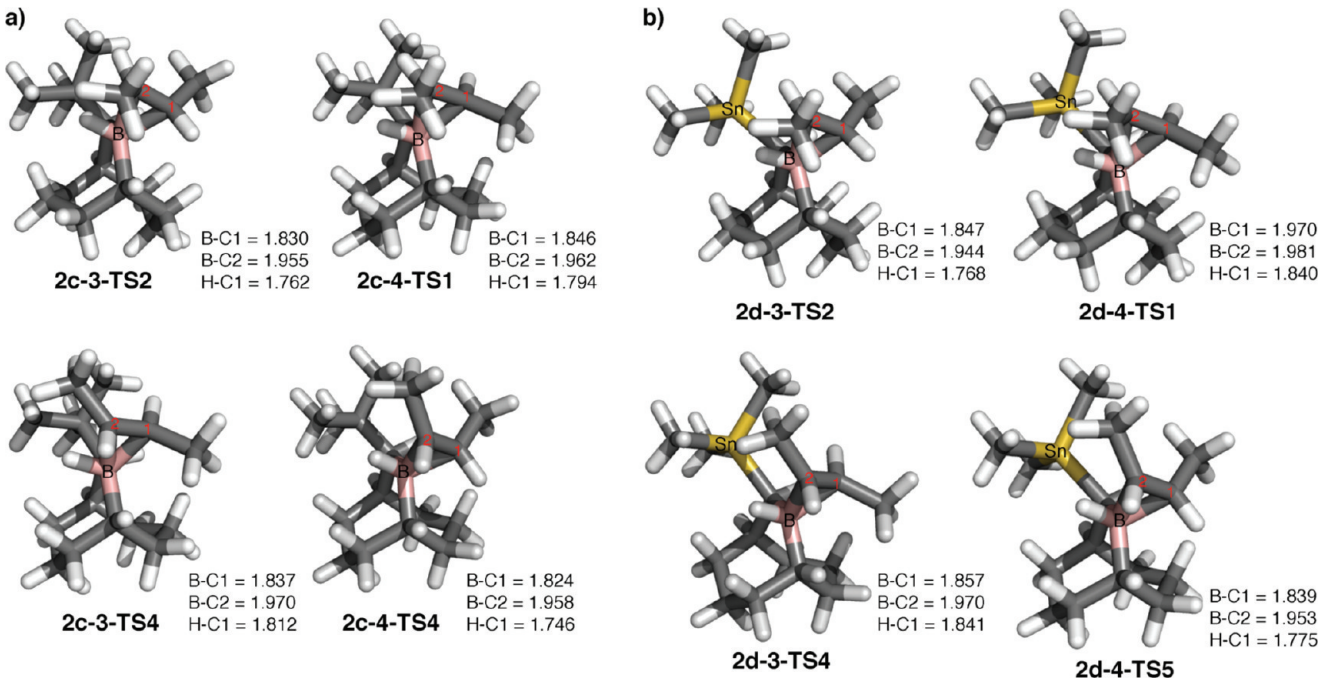

FIGURE 6. Lowest energy B3LYP/6-31G(d,p) hydroboration transition structures for the additions of **2c** and **2d** to alkenes **3** and **4**.

TABLE 5. Activation Energies, Enthalpies, and Free Energies (kcal/mol) for 10-CMe_3-9-borabicyclo[3.3.2]decane (2c) and 10-$SnMe_3$-9-borabicyclo-[3.3.2]decane (2d)[a] after Hydroboration of Alkenes 3 and 4 at 298 K

	$\Delta E^{\ddagger}$	$\Delta H^{\ddagger}$	$\Delta G^{\ddagger}$
structure	B3LYP/6-31G(d,p	B3LYP/6-31G(d,p	B3LYP/6-31G(d,p
2c-3-TS1	17.9	18.0	34.6
2c-3-TS2	17.4	17.5	34.5
2c-3-TS3	19.2	19.4	36.0
2c-3-TS4	21.2	21.3	38.2
2c-3-TS5	22.6	22.8	39.8
2c-3-TS6	22.1	22.2	38.7
2c-4-TS1	16.4	17.9	33.2
2c-4-TS2	17.5	19.1	34.4
2c-4-TS3	17.8	19.4	34.5
2c-4-TS4	19.8	21.3	36.6
2c-4-TS5	20.0	21.5	37.2
2c-4-TS6	20.2	21.7	37.4
2d-3-TS1	20.7	21.8	36.6
2d-3-TS2	20.3	21.4	36.3
2d-3-TS3	23.0	24.1	38.3
2d-3-TS4	24.1	25.3	40.2
2d-3-TS5	25.7	26.8	41.7
2d-3-TS6	25.9	27.0	41.9
2d-4-TS1	20.8	21.8	36.2
2d-4-TS2	21.8	22.8	37.3
2d-4-TS3	22.5	23.6	38.1
2d-4-TS4	21.4	22.3	37.3
2d-4-TS5	21.3	22.2	37.3
2d-4-TS6	23.8	24.9	39.5

[a]For reactions with **2d**, the LACVP** basis set was used to model the Sn atom.

predicted selectivity for **2c** versus **2a** for hydroboration of alkene **4** is the result of the *tert*-butyl group not providing sufficient cavity space for the distal alkene methyl group to fit into.[24]

In contrast, reagent **2d** with a 10-$SnMe_3$ group is predicted to give high ee (> 99%) with alkene **3** and very poor ee with alkene **4** (22%). The smallest $\Delta\Delta E^{\ddagger}$ between favored and unfavored enantiomeric pathways are 3.4 and 0.6 kcal/mol for **2c** and **2d**, respectively. Here the very long C−$SnMe_3$ bond provides too large of a cavity and the alkene methyl group experiences little repulsion. Figure 7 shows space-filling models of optimized **2a**, **2c**, and **2d**. It is evident from these space-filling models that there is essentially no cavity in **2c**, a small cavity in **2a**, and a large cavity in **2d**. This nicely explains the decreasing order of enantioselectivity for the hydroboration of *cis*-alkene **4**.

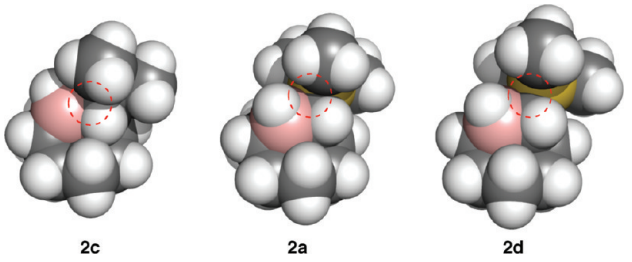

FIGURE 7. Space-filling models of **2c**, **2a**, and **2d** showing the binding pocket area highlighted by the red dashed circle.

10-TMS-9-borabicyclo[3.3.2]decane Hydroboration of 1,1-Disubstituted Alkene 5. Reagent **2a** is highly novel because it also induces a moderate 52% ee for reaction with alkene **5**. Typically, reagents that induce high ee with either *cis*- or *trans*-alkenes result in very poor or no ee with *gem*-disubstituted alkenes. Figure 8 shows the computed transition structures for hydroboration of **5** with **2a**. The overall lowest energy transition structure is for *pro-R* face BH addition, **2a-5-TS2**, with an activation energy of 19.0 kcal/mol ($\Delta E^{\ddagger}_{SCS\text{-}MP2}$ = 11.3 kcal/mol); see Table 6. In this favored enantiomeric transition state, the bulkier isopropyl group is

(24) Although **2c** is predicted to give better ee values than **2a** for hydroboration of alkenes **3** and **4**, it is not superior for hydroboration of alkene **5**, which is predicted to give an ee value of nearly zero (see the Supporting Information).

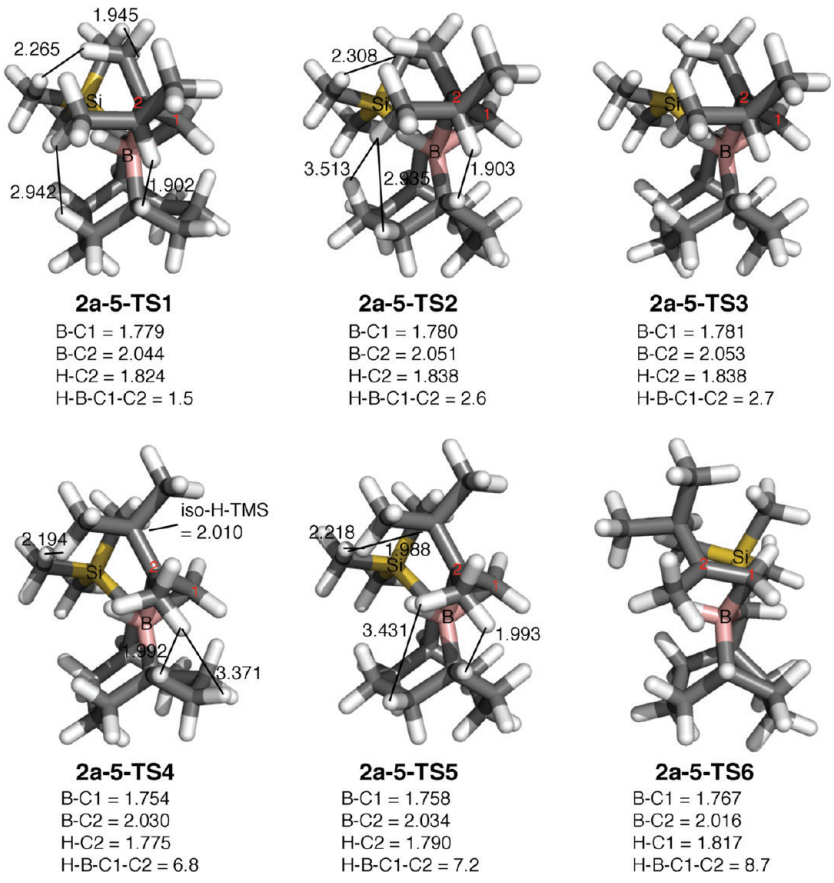

FIGURE 8. B3LYP/6-31G(d,p) hydroboration transition structures for **2a** with alkene **5**.

TABLE 6. Activation Energies, Enthalpies, and Free Energies (kcal/mol) for 2a Addition to 5 at 298 K

	$\Delta E^{\ddagger}$		$\Delta H^{\ddagger}$	$\Delta G^{\ddagger}$
structure	B3LYP/ 6-31G(d,p)	SCS-MP2/ 6-31G(d,p)	B3LYP/ 6-31G(d,p)	B3LYP/ 6-31G(d,p)
2a-5-TS1	20.2	12.2	21.1	36.7
2a-5-TS2	19.0	11.3	19.9	34.9
2a-5-TS3	21.8	15.6	22.9	37.3
2a-5-TS4	19.5	12.2	20.4	35.6
2a-5-TS5	20.1	12.2	21.0	36.5
2a-5-TS6	20.5	12.0	21.5	36.9

directed away from the 10-TMS group while the methyl group is directed toward the 10-TMS group. However, this is not general. For the same borabicyclo ring conformation only **2a-5-TS2** is lower than **2a-5-TS5**. **2a-5-TS4** is lower in energy than **2a-5-TS1** ($\Delta\Delta E^{\ddagger}$ = 0.7 kcal/mol) and **2a-5-TS6** is lower in energy than **2a-5-TS3** ($\Delta\Delta E^{\ddagger}$ = 1.3 kcal/mol). This results in a decrease of the π-facial selectivity.

For *pro-S* face hydroboration, **2a-5-TS4** is lowest in energy and only 0.5 kcal/mol above **2a-5-TS2**. There is also a large regioselective preference of ~6 kcal/mol (see the Supporting Information). Although there is a consensus by both DFT and ab initio methods that **2a-5-TS2** is lowest overall in energy, for the unfavored *pro-S* face transition states, B3LYP predicts **2a-5-TS4** to be lower than **2a-5-TS5** and **2a-5-TS6**, whereas SCS-MP2 predicts **2a-5-TS6** to be lower than **2a-5-TS4** and **2a-5-TS5**; see Table 6. Based on transition-state ensembles of activation energies, B3LYP and SCS-MP2 underestimate enantioselectivity with predicted values of 26% and 24% compared to the experimental 52%. Using B3LYP free energies gives a more accurate predicted enantioselectivity of 45% (see Table 8).

10-Phenyl-9-borabicyclo[3.3.2]decane Hydroboration of Alkenes 3−5. For alkenes **3**−**5**, the 10-phenyl reagent **2b** induces ee comparable to that from **2a** for only *trans*-alkene **3**. Hydroboration of alkenes **4** and **5** with **2b** results in much lower ee values than with **2a**. Figure 9 shows only the lowest energy transition structures for each enantiomeric pathway for **2b** addition to alkenes **3**−**5**. Table 7 gives the computed activation energies for all transition structures.

In accord with the selectivity model proposed by Soderquist and co-workers, the lowest energy transition structures all have the 3-position methylene directed up toward the alkene and the 7-position methylene group directed away from the alkene and correspond to the ground-state conformation **2b-CF1**. The opposite chair/boat transition structure conformations are 1−3 kcal/mol higher in energy (see Table 7 for energies and the Supporting Information for structures).

Transition-state calculations for the hydroboration of propene by **2b** reveals that the alkene methyl group closest to the 10-Ph group induces 0.7 kcal/mol of selectivity. In **2b-3-TS1**, this methyl group is directed away from the phenyl π-face, and the vinyl hydrogen interacts with the phenyl π-face at a distance of 2.956 Å to the C_A phenyl carbon.

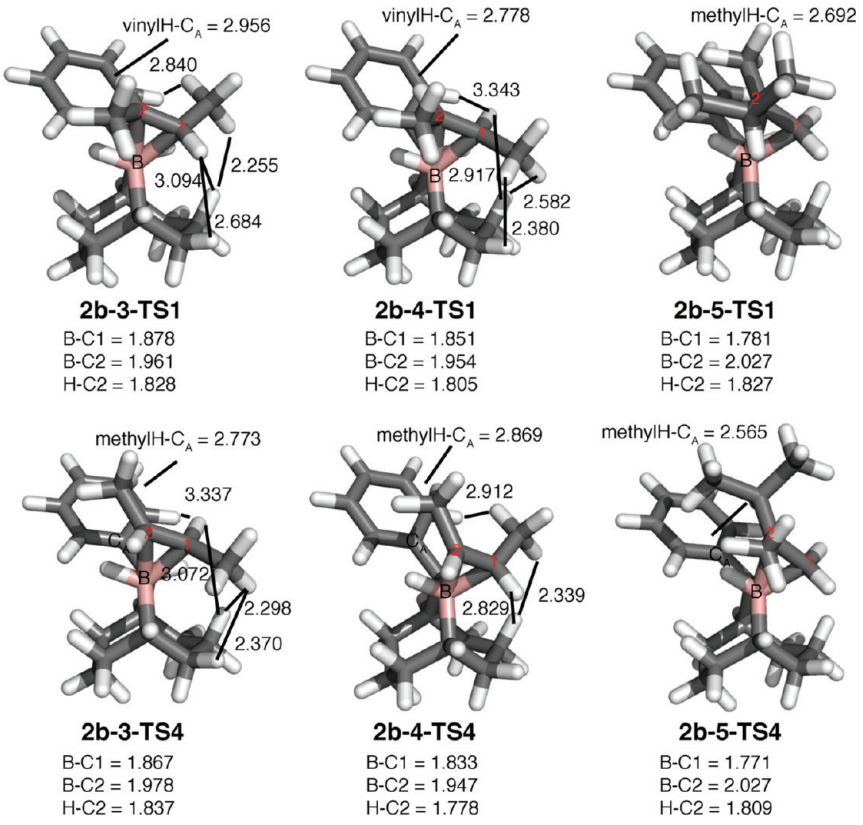

FIGURE 9. Lowest energy hydroboration transition structures (B3LYP/6-31G(d,p)) for reaction of **2b** with alkenes **3**−**5**

TABLE 7. Activation Energies, Enthalpies, and Free Energies (kcal/mol) for 2b Addition to Alkenes 3−5 at 298 K

	$\Delta E^{\ddagger}$		$\Delta H^{\ddagger}$	$\Delta G^{\ddagger}$
structure	B3LYP/6-31G(d,p)	SCS-MP2/6-31G(d,p)	B3LYP/6-31G(d,p)	B3LYP/6-31G(d,p)
2b-3-TS1	9.5	0.5	11.2	26.5
2b-3-TS2	10.6	2.0	12.2	27.3
2b-3-TS3	10.8	2.4	12.4	27.5
2b-3-TS4	11.8	2.9	13.5	28.7
2b-3-TS5	13.6	4.9	15.3	30.4
2b-3-TS6	13.5	5.1	15.1	30.0
2b-4-TS1	9.2	−0.2	10.7	26.2
2b-4-TS2	10.5	1.5	12.0	27.3
2b-4-TS3	11.3	2.8	12.8	28.0
2b-4-TS4	9.2	0.5	10.8	25.8
2b-4-TS5	10.8	2.6	12.4	27.1
2b-4-TS6	10.7	2.3	12.3	27.1
2b-5-TS1	7.5	−1.4	8.7	24.6
2b-5-TS2	9.2	0.7	10.5	25.8
2b-5-TS3	10.1	2.4	11.5	26.9
2b-5-TS4	8.1	0.7	9.3	25.3
2b-5-TS5	9.4	0.7	10.6	26.3
2b-5-TS6	10.3	1.2	11.6	27.2

In **2b-3-TS4**, the methyl group-C_A phenyl carbon distance is 2.773 Å. Estimated by the propene transition structures, the distal methyl group induces 0.9 kcal/mol of selectivity. Again, this methyl group prefers to be on the same side as the 10-Ph group because the phenyl ring is able to rotate and provide a space for the methyl group which allows relief of repulsive interactions with the 2- and 3-position methylene groups.

For the hydroboration of *cis*-alkene **4**, these methyl group selectivity effects cancel and lead to poor enantioselectivity. For example, in **2b-4-TS1** the distance between the distal methyl group and the 2-position methylene hydrogen is 2.380 Å and the 3-position hydrogen is 2.582 Å. The 2-position interaction is alleviated in **2b-4-TS4**, but now the other *cis*-methyl group interacts directly with the 10-Ph group at a distance of 2.869 Å. Also, in **2b-4-TS4**, the distance between the methyl group and 3-position methyl group decreases to 2.339 Å, rather than increases. B3LYP predicts equivalent activation energies for **2b-4-TS1** and **2b-4-TS4**, while SCS-MP2 predicts a 0.7 kcal/mol energy difference. However, SCS-MP2 predicts **2b-4-TS1** to be lower in energy than **2b-4-TS4**. This prediction is in opposition to the experimentally observed alcohol product enantiomeric excess. Although **2b-4-TS1** is favored over **2b-4-TS4** using electronic energy and enthalpy differences, the selectivity is correctly predicted when free energies are used (see Table 7). The $\Delta\Delta G^{\ddagger}$ between **2b-4-TS1** and **2b-4-TS4** is −0.4 kcal/mol. This is also true for the two other borabicyclo ring conformations. The $\Delta\Delta G^{\ddagger}$ between **2b-4-TS2**/**2b-4-TS5** and **2b-4-TS3**/**2b-4-TS6** are −0.2 and −0.9 kcal/mol, respectively.

TABLE 8. Summary of Predicted versus Experimental Enantiomeric Excess (%)

reaction	experiment	B3LYP[a]	SCS-MP2
2a + **3**	95	99 (99)	99
2a + **4**	84	94 (85)	89
2a + **5**	52	26 (45)	24
2b + **3**	96	96 (96)	97
2b + **4**	32	0 (33)	53[b]
2b + **5**	38	44 (51)	87

[a]Values in parentheses are predicted on the basis of $\Delta G^{\ddagger}$ values. All other values are based on $\Delta E^{\ddagger}$ values. [b]Predicts opposite enantiomer from experiment.

These free energies (as well as activation energies) show that largest selectivity occurs when the 7-position and 3-position methylene groups are directed away from the alkene, indicating that the 3-position may be less important than the 2-position methylene group. Based on the transition-state free energies, B3LYP predicts a 33% ee value for the reaction of **2b** with *cis*-alkene **4**. This is remarkably close to the experimental 32% ee value measured experimentally. For reactions of **2b** with alkenes **3** and **5**, 97% and 44% ee values, were predicted.

Predicted versus Experimental Enantioselectivity. In general, B3LYP and SCS-MP2 methods predict enantiomeric excess in close agreement with experiment. Table 8 compares the predicted and experimental ee values. It is clear that the use of B3LYP $\Delta G^{\ddagger}$ values gives the closest agreement with experiment. For hydroboration reactions with reagent **2a**, all methods overestimate selectivity with *trans*-alkene **3** but do correctly predict the drop in selectivity with *cis*-alkene **4**. For the reaction of **2a** with alkene **5**, the use of electronic energies provides too low of an estimate of ee and only B3LYP free energies give a reasonable predicted ee value.

For reactions with reagent **2b**, all methods closely model the 96% ee observed for hydroboration of alkene **3**. The hydroboration of alkene **4** by **2b** was the most difficult to model. Activation energies predict the incorrect favored transition state, and only the use of B3LYP free energies gives a value in accord with experiment. For the reaction of **2a** with alkene **5**, only the SCS-MP2 method predicts a value significantly different than experiment.

4. Conclusion

DFT and ab initio methods were used to analyze alkene hydroboration transition structures for 10-R-9-borabicyclo-[3.3.2]decane reagents. Transition-state ensembles quantitatively modeled enantioselectivity in excellent agreement with experiment, especially using B3LYP free energies. The 10-R group and its conformation is more important than the exact borabicyclo chair/boat ring conformation. This was supported by calculations that compared 10-*tert*-butyl, 10-TMS, and 10-$SnMe_3$ groups, which show that a 10-R binding cavity allows relief of steric repulsion between alkene methyl group with the bridgehead CH bond and the 2- and 3-position methylene groups.

Acknowledgment. This work was supported by the NIH (GM038436 and GM026782) and a postdoctoral fellowship to J.K. from the Ministère des Affaires Etrangères et Européennes (France).

Supporting Information Available: Cartesian coordinates and absolute energies.This material is available free of charge via the Internet at http://pubs.acs.org.